Received: 8 October 2020 | Accepted: 13 April 2022

DOI: 10.1002/rnc.6168

RESEARCH ARTICLE

WILEY

State observers for the time discretization of a class of impulsive mechanical systems

Pascal V. Preiswerk | **Remco I. Leine**

Institute for Nonlinear Mechanics, University of Stuttgart, Stuttgart, Germany

Correspondence
Pascal V. Preiswerk, Institute for Nonlinear Mechanics, University of Stuttgart, Pfaffenwaldring 9, 70569 Stuttgart, Germany.
Email: preiswerk@inm.uni-stuttgart.de

Abstract

In this work, we investigate the state observer problem for linear mechanical systems with a single unilateral constraint, for which neither the impact time instants nor the contact distance is explicitly measured. We propose to attack the observer problem by transforming and approximating the original continuous-time system by a discrete linear complementarity system (LCS) through the use of the Schatzman–Paoli scheme. From there, we derive a deadbeat observer in the form of a linear complementarity problem. Sufficient conditions guaranteeing the uniqueness of its solution then serve as observability conditions. In addition, the discrete adaptation of an existing passivity-based observer design for LCSs can be applied. A key point in using a time discretization is that the discretization acts as a regularization, that is, the impacts take place over multiple time steps (here two time steps). This makes it possible to render the estimation error dynamics asymptotically stable. Furthermore, the so-called peaking phenomenon appears as singularity within the time discretization approach, posing a challenge for robust observer design.

KEYWORDS

impacts, linear complementarity systems, nonsmooth systems, peaking phenomenon, unilateral constraints

1 | INTRODUCTION

In this work, we will investigate the state observer problem for mechanical systems with impulsive motion, that is, systems with state jumps caused by unilateral constraints, without explicitly measuring the impact time instants. It is an important aspect for the state observer design for systems with state jumps whether or not the time instants at which the state jumps occur are known. Most proposed observers assume that these impact time instants can directly be extracted from measurements, for example, by measuring all relevant positions in a system[1-3] or by directly measuring the presence of contact through contact or tactile sensors.[4] This allows for the design of a state observer that exhibits state jumps at the exact same time instants as the observed system. By exploiting the assumption of maximal monotonicity of the impact law, it is then possible to construct a Lyapunov function for the error dynamics (i.e., the time evolution of the difference between the estimated state and the actual state) which does not increase over impacts. Simply put, the observer problem then reduces to stabilizing the error dynamics for the non-impulsive motion (restricted to the constructed Lyapunov function).

Only few attempts have been made to design state observers in the case of unknown impact time instants. The main difficulty for observer design with unknown impact time instants is that the state jumps of the observed system and the state observer do not coincide.[5,6] This results in the peaking phenomenon: even if the observer state nearly matches the real state, a slight mismatch in the impact time instants leads to a temporarily large Euclidean velocity error caused by velocity jumps.[7-10] The peaking phenomenon makes it difficult to show the asymptotic stability of the error dynamics based on Lyapunov's direct method. One approach for such systems is to find a state transformation that transforms the original system into a new system without state jumps, for which conventional state observer techniques can be applied.[5,6] However, such a transformation does not always exist and is in general difficult to find. Another approach is to introduce a distance metric that gives a distance between two states (such as from the observed system and a state observer), but does not change its value over state jumps.[8] Such a distance metric that is "blind" to state jumps can be used together with suitable stability notions (see, e.g., Reference 11 for definitions of incremental stability for hybrid systems) to find a corresponding Lyapunov function. These approaches have been shown to be useful to solve the tracking problem[7] or for controlled synchronization,[12] where all states are known. However, they do not imply a suitable state observer design and calculations can be cumbersome.

The starting point of our article is that we recognize two main hurdles which are inherent to the problem of observer design for unilaterally constrained mechanical systems. The first problem is the simple fact that jumps in the state, occurring in a continuous-time system, generally form a hurdle for Lyapunov-type analysis and thereby for observer design. The second problem is related to the impact law describing the velocity jump in unilaterally constrained systems and this problem needs more explanation. Instantaneous impact laws such as Newton's or Poisson's impact law[13,14] are formulated on velocity level, that is, they directly relate post-impact relative velocities to pre-impact relative velocities. These impact laws, which classically have been defined for systems with a single unilateral constraint, need to be generalized to multiple unilateral constraints (being a topic of active research in the Nonsmooth Dynamics community, see, e.g., References 15 and 16). Generalized versions of these impact laws distinguish between superfluous unilateral constraints which, although closed, do not participate in the impact process, and actively participating unilateral constraints. The combined active-inactive behavior of generalized impact laws on velocity level is conveniently expressed through set-valued functions, for example, normal cone inclusions, which enjoy the favorable property of maximal monotonicity (being related to, but in some sense more strong than, dissipativity of the impact law[17]). Maximal monotonicity of force laws or impact laws leads to contraction properties, which in essence are favorable for tracking or observer design. However, and here lies the problem, the generalized impact laws are only to be applied to *closed* unilateral constraints (i.e., when contact is present). Instantaneous impact laws for multibody systems are therefore formulated on position-switched velocity level. The switching on position level (from closed to open and vice versa) destroys the favorable properties of these impact laws, making the observer design of unilaterally constrained mechanical systems an incredibly difficult task. These two key problems, state jumps and loss of maximal monotonicity of the impact law, explain why the observer design of this class of systems is a Herculean task and risks to reach a dead end.

In this article, we deliberately choose to follow a very different approach, keeping the two key problems right before our eyes. First, instead of analyzing the continuous-time problem with state jumps, we will use a numerical scheme to transform the system to a discrete-time system, approximating the former depending on the chosen time step. The time discretization sidesteps the problem of state jumps as a discrete system only describes state updates over time steps. Moreover, a digital implementation of an observer always needs to be in discrete-time. The time-stepping scheme of Moreau[18] (see also References 9 and 19) is perhaps the most celebrated (velocity-impulse-based) scheme within the Nonsmooth Dynamics community as it can be applied to the simulation of systems with multiple unilateral constraints with Coulomb friction. The Moreau scheme directly discretizes the equality of measures, which describes the system dynamics, and the combined contact-impact law, thereby inheriting the switching nature of the generalized Newtonian impact law. More precisely, in the Moreau scheme one calculates in each time step an index set $\mathcal{J}$ of closed (or penetrating) unilateral constraints to evaluate the combined contact-impact law on velocity level. The Moreau scheme has been successfully used in the simulation of, for example, granular media,[20] masonry structures,[21] robotic systems,[22] human hair movements and circuit breakers. In fact, the Moreau scheme (and extensions thereof, such as the nonsmooth generalized α-method) is the preferred "working horse" in almost all applications. However, regarding the second key problem, we will make use of a less known (and somewhat exotic) time discretization of Schatzman and Paoli,[23,24] which involves an impact law directly formulated on position level, instead of on position-switched velocity level. Thereby the problem of switching of the impact law on position level is circumvented, giving access to the maximal monotonicity property and its related contraction property. The aim of this article is to investigate if this approach is useful to solve the observer design problem of unilaterally constrained mechanical systems without measuring impact time instants.

A related area of research is the design of observers within the switched systems framework, that is, for systems whose dynamics are described by a set of subsystems and a switching law describing how to switch between them. The switching can depend on the value of an external switching signal, in which case a distinction is made between known and unknown switching signals (with unknown switching signals making the design of observers more difficult). To name just a few examples, the works[25,26] investigate systems with an external switching signal. In other cases, the switching is state dependent.[27,28] Even though these works are not concerned with impulsive motion (i.e., with state jumps), they are related to our work. More precisely, we will transform our system to a discrete-time system, which can be recast as a piecewise affine system where the switching is state and input dependent.

The outline is as follows. In Section 2, we formulate the continuous-time observer problem. Based on the Schatzman–Paoli scheme, a suitable time discretization is then derived in Section 3. Subsequently, a deadbeat observer for the discrete observer problem is presented in Section 4. Furthermore, a passivity-based observer design for linear complementarity systems is transported to the discrete-time setting in Section 5. Finally, numerical results for an impact oscillator system are given in Section 6. The usefulness of the presented approach is discussed in Section 7.

2 | CONTINUOUS-TIME STATE OBSERVER PROBLEM

In the following, we will consider a linear mechanical system with f degrees of freedom which is subjected to unilateral constraints (linearity refers to the dynamics in the absence of impacts). Let $\mathbf{q}(t) \in \mathbb{R}^f$ be the generalized coordinates parameterized by the time t and let $\mathbf{u}(t)$ denote the corresponding generalized velocities. Due to the unilateral constraints, discontinuities in the generalized velocities may occur (caused by collisions). In order to allow for discontinuous $\mathbf{u}(t)$, we assume that the generalized velocities are special functions of locally bounded variation, written as $\mathbf{u} \in \mathrm{SLBV}(\mathbb{R}; \mathbb{R}^f)$. Here, $\mathrm{SLBV}(\mathbb{R}; \mathbb{R}^f)$ refers to the subspace of all functions $\boldsymbol{\varphi} : \mathbb{R} \to \mathbb{R}^f$ of locally bounded variation whose Cantor part of the derivative vanishes.[29] It is known that every $\mathbf{u} \in \mathrm{SLBV}(\mathbb{R}; \mathbb{R}^f)$ can be decomposed into an absolutely continuous part $\mathbf{u}_{\mathrm{ac}}$ and a step function $\mathbf{u}_{\mathrm{s}}$ as $\mathbf{u} = \mathbf{u}_{\mathrm{ac}} + \mathbf{u}_{\mathrm{s}}$. Clearly, functions $\mathbf{u} \in \mathrm{SLBV}(\mathbb{R}; \mathbb{R}^f)$ are not differentiable in the classical sense, as step functions are not differentiable at their points of discontinuity. However, such functions can be expressed as integrals, which provide a derivative in the sense of measures. More precisely, with every function of bounded variation $\mathbf{u}$, a differential measure (also called Stieltjes measure) is associated, written as $\mathrm{d}\mathbf{u}$.[30] The integral over a compact interval $[t_a, t_b]$ with respect to the differential measure $\mathrm{d}\mathbf{u}$ is given by

$$\int_{[t_a,t_b]} \mathrm{d}\mathbf{u} = \mathbf{u}^+(t_b) - \mathbf{u}^-(t_a), \tag{1}$$

where $\mathbf{u}^-(t)$ and $\mathbf{u}^+(t)$ denote the left and right limit of $\mathbf{u}$ at t. In the special case of the integration interval being a singleton, that is, $t_a = t_b$, the integral is equal to $\mathbf{u}^+(t_a) - \mathbf{u}^-(t_a)$, being the jump in $\mathbf{u}(t)$ at $t = t_a$. For a more extensive treatment of differential measures and their application to mechanical systems, the reader is referred to References 18, 30, and 31.

The integral in (1) can be divided into two parts. On one hand, we can express a step function as an integral with respect to the Dirac point measure $\mathrm{d}\delta_{t_k}$, which is such that

$$\delta_{t_k}([t_a, t_b]) = \int_{[t_a,t_b]} \mathrm{d}\delta_{t_k} = \begin{cases} 1 & \text{if } \; t_k \in [t_a, t_b], \\ 0 & \text{if } \; t_k \notin [t_a, t_b]. \end{cases} \tag{2}$$

For example, by setting $t_a = 0$ and $t_b = t$, the integral in (2) describes the unit step function h_{t_k} given by $h_{t_k}(t) = 1 \; \forall \; t \geq t_k$ and $h_{t_k}(t) = 0 \; \forall \; t < t_k$. More generally, for a step function $\mathbf{u}_{\mathrm{s}} : \mathbb{R} \to \mathbb{R}^f$ with a countable number of discontinuities at $t_k \in \{t_1, t_2, \dots\}$ and given step heights $\mathbf{u}_{\mathrm{s}}^+(t_k) - \mathbf{u}_{\mathrm{s}}^-(t_k)$ we can write

$$\mathbf{u}_{\mathrm{s}}^+(t_b) = \mathbf{u}_{\mathrm{s}}^-(t_a) + \int_{[t_a,t_b]} (\mathbf{u}_{\mathrm{s}}^+ - \mathbf{u}_{\mathrm{s}}^-) \mathrm{d}\eta, \tag{3}$$

where we used $\mathrm{d}\eta = \sum_k \mathrm{d}\delta_{t_k}$ for brevity. On the other hand, for an absolutely continuous function $\mathbf{u}_{\mathrm{ac}}$ it holds that

$$\mathbf{u}_{\mathrm{ac}}^+(t_b) = \mathbf{u}_{\mathrm{ac}}^-(t_a) + \int_{[t_a,t_b]} \dot{\mathbf{u}}_{\mathrm{ac}} \mathrm{d}t, \tag{4}$$

where $\dot{\mathbf{u}}_{\mathrm{ac}} := \mathrm{d}\mathbf{u}_{\mathrm{ac}}/\mathrm{d}t$ denotes the time derivative and $\mathrm{d}t$ is the Lebesgue measure on $\mathbb{R}$, leading to the continuity property $\mathbf{u}_{\mathrm{ac}}^{+}(t_a) - \mathbf{u}_{\mathrm{ac}}^{-}(t_a) = \mathbf{0}$. Adding both sides of (3) and (4) and using the decomposition $\mathbf{u} = \mathbf{u}_{\mathrm{ac}} + \mathbf{u}_{\mathrm{s}}$ leads to

$$\mathbf{u}^{+}(t_b) - \mathbf{u}^{-}(t_a) = \int_{[t_a,t_b]} \dot{\mathbf{u}}_{\mathrm{ac}} \mathrm{d}t + \int_{[t_a,t_b]} (\mathbf{u}_s^{+} - \mathbf{u}_s^{-}) \mathrm{d}\eta. \tag{5}$$

Note that $\mathbf{u}^{+} - \mathbf{u}^{-} = \mathbf{u}_{\mathrm{s}}^{+} - \mathbf{u}_{\mathrm{s}}^{-}$ because $\mathbf{u}_{\mathrm{ac}}$ is continuous and $\dot{\mathbf{u}} = \dot{\mathbf{u}}_{\mathrm{ac}}$ wherever it is defined since $\mathbf{u}_{\mathrm{s}}$ is constant between points of discontinuity. Therefore, by applying (1) to the left-hand side of (5), it follows that

$$\int_{[t_a,t_b]} \mathrm{d}\mathbf{u} = \int_{[t_a,t_b]} \dot{\mathbf{u}} \mathrm{d}t + (\mathbf{u}^{+} - \mathbf{u}^{-}) \mathrm{d}\eta, \tag{6}$$

or, written as an equality of measures, $\mathrm{d}\mathbf{u} = \dot{\mathbf{u}}\mathrm{d}t + (\mathbf{u}^{+} - \mathbf{u}^{-})\mathrm{d}\eta$.

The dynamics of a linear mechanical system which is subjected to unilateral constraints is described by a measure differential inclusion of the form[9]

$$\begin{aligned} \mathrm{d}\mathbf{q} &= \mathbf{u}\mathrm{d}t, \\ \mathbf{M}\mathrm{d}\mathbf{u} + (\mathbf{K}\mathbf{q} + \mathbf{D}\mathbf{u} - \mathbf{f}(t))\mathrm{d}t &= \mathbf{W}\mathrm{d}\mathbf{P}, \end{aligned} \tag{7}$$

where $\mathrm{d}\mathbf{q}$ is the differential measure of the generalized coordinates $\mathbf{q}$, $\mathrm{d}\mathbf{u} = \dot{\mathbf{u}}\mathrm{d}t + (\mathbf{u}^{+} - \mathbf{u}^{-})\mathrm{d}\eta$ is the differential measure of the generalized velocities, allowing for discontinuities in the generalized velocities $\mathbf{u}$. Furthermore, $\mathrm{d}\mathbf{P} = \boldsymbol{\lambda}\mathrm{d}t + \boldsymbol{\Lambda}\mathrm{d}\eta$ is the differential contact effort measure. More precisely, $\boldsymbol{\lambda}$ model the constraint forces during the non-impulsive motion and $\boldsymbol{\Lambda}$ are the impulsive forces due to impacts. The system is subjected to a bounded, time-dependent external forcing $\mathbf{f}(t)$. For the sake of simplicity, we assume that the mass matrix $\mathbf{M}$, the stiffness matrix $\mathbf{K}$, and the damping matrix $\mathbf{D}$ are constant. Furthermore, the unilateral constraints are described by linear inequality conditions $\mathbf{g}(\mathbf{q}) = \mathbf{W}^{\mathsf{T}}\mathbf{q} \geq 0$ and the generalized force directions, given by the columns of $\mathbf{W} = (\partial \mathbf{g}/\partial \mathbf{q})^{\mathsf{T}}$, are assumed to be constant and linearly independent ($\mathbf{W}$ has full rank).

For the components of the constraint forces $\boldsymbol{\lambda}$ and $\boldsymbol{\Lambda}$, we assume Signorini's law on position level

$$0 \leq \mathbf{g} \perp \boldsymbol{\lambda} \geq 0, \tag{8a}$$

$$0 \leq \mathbf{g} \perp \boldsymbol{\Lambda} \geq 0, \tag{8b}$$

where we used the notation $\boldsymbol{g} \geq 0$ to express that every component $g_i \geq 0 \forall i$ and the notation $\boldsymbol{g} \perp \boldsymbol{\lambda}$ to express the orthogonality $\boldsymbol{g}^{\mathsf{T}}\boldsymbol{\lambda} = 0$. Hence, (8a) is equivalent to $g_i \geq 0, \lambda_i \geq 0, g_i\lambda_i = 0$ for all i and is therefore referred to as an inequality complementarity. The constraint forces can alternatively be formulated on position-switched velocity level. With $\boldsymbol{\gamma} = \mathbf{W}^{\mathsf{T}}\mathbf{u}$ we then have component-wise

$$\begin{aligned} g_i(\mathbf{q}) = 0 &: 0 \leq \gamma_i \perp \lambda_i \geq 0\,, \quad g_i(\mathbf{q}) > 0 : \lambda_i = 0, \\ g_i(\mathbf{q}) = 0 &: 0 \leq \gamma_i \perp \Lambda_i \geq 0\,, \quad g_i(\mathbf{q}) > 0 : \Lambda_i = 0. \end{aligned} \tag{9}$$

In addition to the force laws, an impact law has to be specified for a full description of the dynamics. Here, we will make use of a generalized Newtonian impact law,[13] which is written component-wise as

$$\begin{aligned} g_i(\mathbf{q}) = 0 &: \; 0 \leq \xi_i \perp \Lambda_i \geq 0, \\ g_i(\mathbf{q}) > 0 &: \; \Lambda_i = 0, \end{aligned} \tag{10}$$

with the kinematic variable $\xi_i := \gamma_i^{+} + \varepsilon\gamma_i^{-}$ and a given coefficient of restitution $\varepsilon \in [0, 1]$. The force law (9) and the impact law (10) can be gathered in a description of measures

$$\begin{aligned} g_i(\mathbf{q}) = 0 &: \; 0 \leq \xi_i \perp \int_{\mathcal{I}} \mathrm{d}P_i \geq 0, \\ g_i(\mathbf{q}) > 0 &: \; \int_{\mathcal{I}} \mathrm{d}P_i = 0, \end{aligned} \tag{11}$$

where the sign (or nullity) of g_i and ξ_i is assumed to be constant during the interval $\mathcal{I}$ (e.g., a short time step as used in a time discretization). For brevity, (11) is usually written as

$$\begin{aligned} g_i(\mathbf{q}) = 0 &: \ 0 \leq \xi_i \perp \mathrm{d}P_i \geq 0, \\ g_i(\mathbf{q}) > 0 &: \ \mathrm{d}P_i = 0, \end{aligned} \tag{12}$$

refraining from referring to the assumption on $\mathcal{I}$.

The question is now, given the system dynamics as a measure differential inclusion (7) together with the force laws and an impact law, how can we design a state observer, that recovers all positions and velocities from measurements? Even though the dynamics is linear in the absence of impacts, this is not a trivial task. Several observer designs are available in the literature, which assume that contact information is known through measurement, that is, the index set of closed unilateral constraints $\mathcal{J} = \{i | g_i = 0\}$ is measured through contact sensors. What these observer designs have in common is that they consist of a copy of the observed system, modified such that the observer closes its unilateral constraints depending on the measurement signals. Furthermore, Luenberger-type correction terms and in some cases position jumps are added. As an example, in Reference 1, a minimal order velocity observer of the form (adapted to our notation)

$$\begin{aligned} &\mathbf{M}\mathrm{d}\mathbf{z} - (\mathbf{D}\hat{\mathbf{u}} + \mathbf{K}\mathbf{q} - \mathbf{f}(t))\mathrm{d}t - \mathbf{M}\mathbf{L}\hat{\mathbf{u}}\mathrm{d}t = \mathbf{W}\mathrm{d}\hat{\mathbf{P}}, \\ &\hat{\mathbf{u}} = \mathbf{z} - \mathbf{L}\mathbf{q}, \end{aligned} \tag{13}$$

with the force law

$$\begin{aligned} g_i(\mathbf{q}) = 0 &: \ 0 \leq \hat{\xi}_i \perp \mathrm{d}\hat{P}_i \geq 0, \\ g_i(\mathbf{q}) > 0 &: \ \mathrm{d}\hat{P}_i = 0, \end{aligned} \tag{14}$$

is introduced. Therein, $\mathbf{q}$ is the measured position and quantities with a hat ($\hat{}$) refer to entities of the observer. As the combined contact-impact law (14) switches depending on the measured positions $\mathbf{q}$, impacts in the state observer dynamics occur at the exact same time instants as for the observed system. By exploiting the assumption of maximal monotonicity of the impact law, it is therefore possible to construct a Lyapunov function for the error dynamics to show that the estimated state converges to the actual state. The topic of the present article is to develop methods for observer design *without* contact information.

3 | DISCRETE-TIME STATE OBSERVER PROBLEM

In the following, we pursue an alternative approach, where we first discretize the dynamics and then design a state observer for the discrete (and therefore approximate) system. As explained in the Introduction, this alleviates the problem of state jumps in the observer design.

Here, we will make use of the less known scheme of Schatzman and Paoli.[23,24] Schatzman and Paoli motivated this somewhat exotic scheme, which involves an impact law on position level, by the fact that it allows for a rigorous convergence proof (more rigorous than can be given for the Moreau scheme referred to in the introduction). However, the practical application of this scheme is restricted, as it can only be applied to mechanical systems with a single *frictionless* unilateral constraint, or, more generally, to multiple frictionless unilateral constraints which are decoupled such that $\mathbf{w}_i^{\mathrm{T}}\mathbf{M}^{-1}\mathbf{w}_j = 0$ for $i \neq j$, where $\mathbf{w}_i = \partial g_i / \partial \mathbf{q}$. The Schatzman–Paoli discretization scheme can in our case be written as

$$\begin{aligned} &\mathbf{q}_{k+1} = \mathbf{q}_k + \Delta t \mathbf{u}_{k+1}, \\ &\mathbf{M}(\mathbf{u}_{k+1} - \mathbf{u}_k) + \left(\mathbf{K}\mathbf{q}_k + \mathbf{D}\mathbf{u}_k - \mathbf{f}_k\right)\Delta t = \mathbf{W}\mathbf{P}_k, \end{aligned} \tag{15}$$

together with

$$\begin{aligned}\boldsymbol{\zeta}_k &:= \mathbf{g}_{k+1} + \varepsilon \mathbf{g}_{k-1},\\ 0 \le \boldsymbol{\zeta}_k &\perp \mathbf{P}_k \ge 0,\end{aligned} \tag{16}$$

where Δt is the (constant) time step size and an index k refers to the corresponding variable being evaluated (or approximated) at $t = t_k := k\Delta t$, for example, $\mathbf{q}_k := \mathbf{q}(t_k)$. The above discretization has the form of a semi-implicit Euler scheme, directly applied to the MDI (7). Likewise the discrete contact distance is $\mathbf{g}_k = \mathbf{W}^\mathsf{T}\mathbf{q}_k$ and the corresponding discrete contact velocity is $\boldsymbol{\gamma}_k = \mathbf{W}^\mathsf{T}\mathbf{u}_k$. To keep a simple notation, we will assume all coefficients of restitution $\varepsilon_i = \varepsilon$ to be equal. What makes the Schatzman–Paoli scheme special is the fact that the discrete impact law (16), that is, $0 \le \mathbf{g}_{k+1} + \varepsilon \mathbf{g}_{k-1} \perp \mathbf{P}_k \ge 0$, is formulated on position level, thereby circumventing the calculation of an index set. This discrete impact law may seem somewhat heuristic as it is not a direct discretization of the combined contact-impact law (12). Its meaningfulness becomes clear when evaluated over multiple time steps. Indeed, if $\boldsymbol{\zeta}_k$ vanishes over two consecutive time steps, that is, $\boldsymbol{\zeta}_{k-1} = \boldsymbol{\zeta}_k = \mathbf{0}$, then it follows with the definition of $\boldsymbol{\zeta}_k$ in (16) that

$$\begin{aligned}\frac{\boldsymbol{\zeta}_k - \boldsymbol{\zeta}_{k-1}}{\Delta t} &= \frac{\mathbf{g}_{k+1} - \mathbf{g}_k}{\Delta t} + \varepsilon \frac{\mathbf{g}_{k-1} - \mathbf{g}_{k-2}}{\Delta t} = \mathbf{W}^\mathsf{T}\left(\frac{\mathbf{q}_{k+1} - \mathbf{q}_k}{\Delta t} + \varepsilon \frac{\mathbf{q}_{k-1} - \mathbf{q}_{k-2}}{\Delta t}\right)\\ &= \mathbf{W}^\mathsf{T}(\mathbf{u}_{k+1} + \varepsilon \mathbf{u}_{k-1}) = \boldsymbol{\gamma}_{k+1} + \varepsilon \boldsymbol{\gamma}_{k-1} = \mathbf{0}.\end{aligned} \tag{17}$$

The last equality, $\boldsymbol{\gamma}_{k+1} + \varepsilon \boldsymbol{\gamma}_{k-1} = \mathbf{0}$, shows that Newton's impact law is fulfilled in a discretized sense over two time steps. Velocity jumps that occur instantaneously in continuous time take place over an interval of two time steps in the discretization, which can be seen as a regularization. In the following, let us derive the state-space representation of the discretized system (15), (16) by introducing the state $\mathbf{x}_k := \begin{pmatrix}\mathbf{q}_k^\mathsf{T} & \mathbf{u}_k^\mathsf{T}\end{pmatrix}^\mathsf{T}$. Note that we are writing variables and matrices related to the state-space description without serifs, whereas in our original description of the mechanical system we are using serifs (therefore, variables denoted by the same letter, are assigned a different meaning depending on whether they are written with or without serifs). Rewriting Equation (15) as

$$\begin{pmatrix}\mathbf{I} & -\Delta t\mathbf{I}\\ \mathbf{0} & \mathbf{M}\end{pmatrix}\mathbf{x}_{k+1} = \begin{pmatrix}\mathbf{I} & \mathbf{0}\\ -\Delta t\mathbf{K} & \mathbf{M} - \Delta t\mathbf{D}\end{pmatrix}\mathbf{x}_k + \begin{pmatrix}\mathbf{0}\\ \mathbf{W}\end{pmatrix}\mathbf{P}_k + \begin{pmatrix}\mathbf{0}\\ \Delta t\mathbf{I}\end{pmatrix}\mathbf{f}_k, \tag{18}$$

and inverting the matrix on the left-hand side, yields an update rule for the state

$$\mathbf{x}_{k+1} = \begin{pmatrix}\mathbf{I} & \Delta t\mathbf{M}^{-1}\\ \mathbf{0} & \mathbf{M}^{-1}\end{pmatrix}\left[\begin{pmatrix}\mathbf{I} & \mathbf{0}\\ -\Delta t\mathbf{K} & \mathbf{M} - \Delta t\mathbf{D}\end{pmatrix}\mathbf{x}_k + \begin{pmatrix}\mathbf{0}\\ \mathbf{W}\end{pmatrix}\mathbf{P}_k + \begin{pmatrix}\mathbf{0}\\ \Delta t\mathbf{I}\end{pmatrix}\mathbf{f}_k\right], \tag{19}$$

where $\mathbf{0}$ denotes a zero matrix of appropriate dimensions. Finally, after simple matrix multiplications we arrive at

$$\mathbf{x}_{k+1} = \mathbf{A}\mathbf{x}_k + \mathbf{B}\mathbf{P}_k + \mathbf{E}\mathbf{f}_k, \tag{20}$$

with the corresponding system matrices $\mathbf{A}$, $\mathbf{B}$, and $\mathbf{E}$ given by

$$\mathbf{A} = \begin{pmatrix}\mathbf{I} - \Delta t^2\mathbf{M}^{-1}\mathbf{K} & \Delta t(\mathbf{I} - \Delta t\mathbf{M}^{-1}\mathbf{D})\\ -\Delta t\mathbf{M}^{-1}\mathbf{K} & \mathbf{I} - \Delta t\mathbf{M}^{-1}\mathbf{D}\end{pmatrix}, \quad \mathbf{B} = \begin{pmatrix}\Delta t\mathbf{M}^{-1}\mathbf{W}\\ \mathbf{M}^{-1}\mathbf{W}\end{pmatrix}, \quad \mathbf{E} = \begin{pmatrix}\Delta t^2\mathbf{M}^{-1}\\ \Delta t\mathbf{M}^{-1}\end{pmatrix}. \tag{21}$$

To complete the state-space description, we express the discrete impact law (16) in the state variables. We simply use the contact distance $\mathbf{g}_k = \mathbf{W}^\mathsf{T}\mathbf{q}_k$ and the first equation of (15) as follows in (16)

$$\begin{aligned}\boldsymbol{\zeta}_k &= \mathbf{W}^\mathsf{T}(\mathbf{q}_{k+1} + \varepsilon \mathbf{q}_{k-1}) = \mathbf{W}^\mathsf{T}(\mathbf{q}_{k+1} + \varepsilon(\mathbf{q}_k - \Delta t\mathbf{u}_k))\\ &= \begin{pmatrix}\mathbf{W}^\mathsf{T} & \mathbf{0}\end{pmatrix}\mathbf{x}_{k+1} + \varepsilon\begin{pmatrix}\mathbf{W}^\mathsf{T} & -\Delta t\mathbf{W}^\mathsf{T}\end{pmatrix}\mathbf{x}_k\\ &= \begin{pmatrix}\mathbf{W}^\mathsf{T} & \mathbf{0}\end{pmatrix}\left[\mathbf{A}\mathbf{x}_k + \mathbf{B}\mathbf{P}_k + \mathbf{E}\mathbf{f}_k\right] + \varepsilon\begin{pmatrix}\mathbf{W}^\mathsf{T} & -\Delta t\mathbf{W}^\mathsf{T}\end{pmatrix}\mathbf{x}_k\\ &= \mathbf{C}\mathbf{x}_k + \mathbf{D}\mathbf{P}_k + \mathbf{F}\mathbf{f}_k,\end{aligned} \tag{22}$$

with the matrices

$$\mathbf{C} = \begin{pmatrix} [(1+\varepsilon)\mathbf{I} - \Delta t^2 \mathbf{M}^{-1}\mathbf{K}]^\mathsf{T}\mathbf{W} \\ \Delta t[(1-\varepsilon)\mathbf{I} - \Delta t \mathbf{M}^{-1}\mathbf{D}]^\mathsf{T}\mathbf{W} \end{pmatrix}^\mathsf{T}, \quad \mathbf{D} = \Delta t \mathbf{W}^\mathsf{T}\mathbf{M}^{-1}\mathbf{W}, \quad \mathbf{F} = \Delta t^2 \mathbf{W}^\mathsf{T}\mathbf{M}^{-1}. \tag{23}$$

We recognize the matrix $\mathbf{D}$ above to be a scaled version of the so-called Delassus matrix $\mathbf{W}^\mathsf{T}\mathbf{M}^{-1}\mathbf{W}$,[15] which is symmetric and positive definite as we assume $\mathbf{W}$ to have full column rank. Summarizing the discrete system dynamics (20), (22), and (16) and introducing an output equation $\mathbf{y}_k = \mathbf{G}\mathbf{x}_k$ (i.e., the available measurements) we have

$$\mathbf{x}_{k+1} = \mathbf{A}\mathbf{x}_k + \mathbf{B}\mathbf{P}_k + \mathbf{E}\mathbf{f}_k, \tag{24a}$$

$$\boldsymbol{\zeta}_k = \mathbf{C}\mathbf{x}_k + \mathbf{D}\mathbf{P}_k + \mathbf{F}\mathbf{f}_k, \tag{24b}$$

$$0 \leq \boldsymbol{\zeta}_k \perp \mathbf{P}_k \geq 0, \tag{24c}$$

$$\mathbf{y}_k = \mathbf{G}\mathbf{x}_k, \tag{24d}$$

which is a discrete linear complementarity system (LCS).[32,33] For a given $\mathbf{x}_k$ and $\mathbf{f}_k$, Equations (24b) and (24c) form together a linear complementarity problem (LCP),[34,35] which has to be solved for $\boldsymbol{\zeta}_k$ and $\mathbf{P}_k$ in each time step.

Remark 1. As noted in Reference 24, the time-stepping scheme above admits a unique solution if the set $\mathcal{A} := \{\mathbf{q} \in \mathbb{R}^f | \mathbf{g}(\mathbf{q}) \geq 0\}$ of admissible positions is convex. Here, we restrict ourselves to linear inequality constraints $\mathbf{g}(\mathbf{q}) = \mathbf{W}^\mathsf{T}\mathbf{q}$. It is therefore straightforward to verify that $\mathcal{A}$ is always convex in our setting. Also, the LCP (24b), (24c) has a unique solution if all principal minors of the matrix $\mathbf{D}$ are strictly positive (i.e., it is a so-called $\mathcal{P}$-matrix, see, e.g., Reference 34), which is fulfilled since $\mathbf{D}$ is symmetric and positive definite.

4 | A DISCRETE-TIME DEADBEAT OBSERVER

A state observer that is able to reconstruct the exact state in finite time is commonly called a deadbeat observer. One way to obtain such a deadbeat observer is to simply calculate the state from a collection of known system outputs. Clearly, this method requires exact output measurements and a perfectly accurate model. For discrete linear time invariant systems, one way to calculate the initial state is to propagate the discrete dynamics over $n-1$ steps and to relate it to the measured output in each step. This results in a system of linear equations that can be solved for the initial condition. In the following, we will see that for discrete LCS, it is possible to reconstruct the current state from a number of outputs, by solving a LCP. Sufficient conditions guaranteeing the existence of a unique solution to this LCP then serve as an observability condition. Unsurprisingly, one of these conditions is that the unconstrained motion is observable. In order to use a more standard notation, we will consider a discrete LCS of the form

$$\begin{aligned} \mathbf{x}_{k+1} &= \mathbf{A}\mathbf{x}_k + \mathbf{B}\mathbf{w}_k + \mathbf{E}\mathbf{v}_k, \\ \mathbf{z}_k &= \mathbf{C}\mathbf{x}_k + \mathbf{D}\mathbf{w}_k + \mathbf{F}\mathbf{v}_k, \\ 0 &\leq \mathbf{z}_k \perp \mathbf{w}_k \geq 0, \\ \mathbf{y}_k &= \mathbf{G}\mathbf{x}_k, \end{aligned} \tag{25}$$

with the state $\mathbf{x}_k$, some input $\mathbf{v}_k$, the output $\mathbf{y}_k$, and the complementary variables $\mathbf{z}_k$ and $\mathbf{w}_k$, which play the role of the kinematic variable $\boldsymbol{\zeta}_k$ and the discrete impulse $\mathbf{P}_k$ in (24). For the sake of simplicity, we will restrict ourselves for the moment to the case without external inputs, that is, $\mathbf{v}_k = \mathbf{0}\ \forall\ k$. However, all subsequent steps can straightforwardly be extended to include inputs, as will be discussed in Remark 3. First, we connect the outputs to the initial condition by successively calculating the outputs using (25), that is,

$$\begin{pmatrix}\mathbf{y}_0\\ \mathbf{y}_1\\ \vdots\\ \mathbf{y}_k\end{pmatrix}=\begin{pmatrix}\mathbf{G}\\ \mathbf{GA}\\ \vdots\\ \mathbf{GA}^k\end{pmatrix}\mathbf{x}_0+\begin{bmatrix}\mathbf{0} & \mathbf{0} & \mathbf{0} & \dots & \mathbf{0}\\ \mathbf{GB} & \mathbf{0} & \mathbf{0} & \dots & \mathbf{0}\\ \mathbf{GAB} & \mathbf{GB} & \mathbf{0} & \dots & \mathbf{0}\\ \vdots & & & & \vdots\\ \mathbf{GA}^{k-1}\mathbf{B} & \mathbf{GA}^{k-2}\mathbf{B} & \dots & \mathbf{GB} & \mathbf{0}\end{bmatrix}\begin{pmatrix}\mathbf{w}_0\\ \mathbf{w}_1\\ \vdots\\ \mathbf{w}_k\end{pmatrix}. \tag{26}$$

For a more compact notation we summarize (26) with $\mathbf{Y}_k := \begin{pmatrix}\mathbf{y}_0^\mathsf{T} & \dots & \mathbf{y}_k^\mathsf{T}\end{pmatrix}^\mathsf{T}$ and $\mathbf{W}_k := \begin{pmatrix}\mathbf{w}_0^\mathsf{T} & \dots & \mathbf{w}_k^\mathsf{T}\end{pmatrix}^\mathsf{T}$ in

$$\mathbf{Y}_k = \boldsymbol{\mathcal{O}}_k\mathbf{x}_0 + \mathbf{M}_k\mathbf{W}_k. \tag{27}$$

Similarly, we summarize the corresponding sequence

$$\begin{pmatrix}\mathbf{z}_0\\ \mathbf{z}_1\\ \vdots\\ \mathbf{z}_k\end{pmatrix}=\begin{pmatrix}\mathbf{C}\\ \mathbf{CA}\\ \vdots\\ \mathbf{CA}^k\end{pmatrix}\mathbf{x}_0+\begin{bmatrix}\mathbf{D} & \mathbf{0} & \mathbf{0} & \dots & \mathbf{0}\\ \mathbf{CB} & \mathbf{D} & \mathbf{0} & \dots & \mathbf{0}\\ \mathbf{CAB} & \mathbf{CB} & \mathbf{D} & \dots & \mathbf{0}\\ \vdots & & & & \\ \mathbf{CA}^{k-1}\mathbf{B} & \mathbf{CA}^{k-2}\mathbf{B} & \dots & \mathbf{CB} & \mathbf{D}\end{bmatrix}\begin{pmatrix}\mathbf{w}_0\\ \mathbf{w}_1\\ \vdots\\ \mathbf{w}_k\end{pmatrix}, \tag{28}$$

with $\mathbf{Z}_k = \begin{pmatrix}\mathbf{z}_0^\mathsf{T} & \dots & \mathbf{z}_k^\mathsf{T}\end{pmatrix}^\mathsf{T}$ in the compact form

$$\mathbf{Z}_k = \overline{\boldsymbol{\mathcal{O}}}_k\mathbf{x}_0 + \overline{\mathbf{M}}_k\mathbf{W}_k. \tag{29}$$

Note that matrices with a similar structure are denoted by the same letter, but distinguished by overlines. Since $\mathbf{z}_i$ and $\mathbf{w}_i$ satisfy the inequality complementarity $0 \le \mathbf{z}_i \perp \mathbf{w}_i \ge 0$ for all i, it directly follows that

$$0 \le \mathbf{Z}_k \perp \mathbf{W}_k \ge 0. \tag{30}$$

Finally, propagating the first equation in (25) over k time steps with $\mathbf{v}_k = \mathbf{0}\ \forall\ k$ yields

$$\mathbf{x}_k = \mathbf{A}^k\mathbf{x}_0 + \begin{bmatrix}\mathbf{A}^{k-1}\mathbf{B} & \mathbf{A}^{k-2}\mathbf{B} & \dots & \mathbf{B} & \mathbf{0}\end{bmatrix}\mathbf{W}_k =: \mathbf{A}^k\mathbf{x}_0 + \mathbf{Q}_k\mathbf{W}_k. \tag{31}$$

Now let $k = n-1$ with the number of states n. For a better readability, we will omit all indices if they equal $n-1$. Then, Equations (27), (29), and (30) with known outputs $\mathbf{Y} := \mathbf{Y}_{n-1}$ and the unknown initial state $\mathbf{x}_0$ and contact efforts $\mathbf{W} := \mathbf{W}_{n-1}$ are

$$\begin{aligned}\mathbf{Y} &= \boldsymbol{\mathcal{O}}\mathbf{x}_0 + \mathbf{M}\mathbf{W},\\ \mathbf{Z} &= \overline{\boldsymbol{\mathcal{O}}}\mathbf{x}_0 + \overline{\mathbf{M}}\mathbf{W},\\ 0 &\le \mathbf{Z} \perp \mathbf{W} \ge 0,\end{aligned} \tag{32}$$

and form a mixed linear complementarity problem (MLCP).[36] Our goal is to calculate $\mathbf{x}_0$ and $\mathbf{W}$ for a given $\mathbf{Y}$. The MLCP (32) does have a solution, because it is generated by (24). The matrix $\boldsymbol{\mathcal{O}}$ is the well-known observability matrix for the non-impulsive motion. Therefore, if the system is observable in the absence of impacts, $\boldsymbol{\mathcal{O}}$ has full column rank and the first equation of (32) can uniquely be solved for

$$\mathbf{x}_0 = \boldsymbol{\mathcal{O}}^\dagger[\mathbf{Y} - \mathbf{M}\mathbf{W}], \tag{33}$$

with the left inverse $\boldsymbol{\mathcal{O}}^\dagger$ (which is equal to the inverse $\boldsymbol{\mathcal{O}}^{-1}$ if $\boldsymbol{\mathcal{O}}$ is square). By inserting (33) in the remaining equations of the MLCP we arrive at

$$\begin{aligned}\mathbf{Z} &= \left[\overline{\mathbf{M}} - \overline{\boldsymbol{\mathcal{O}}}\boldsymbol{\mathcal{O}}^{\dagger}\mathbf{M}\right]\mathbf{W} + \overline{\boldsymbol{\mathcal{O}}}\boldsymbol{\mathcal{O}}^{\dagger}\mathbf{Y},\\ 0 &\leq \mathbf{Z} \perp \mathbf{W} \geq 0,\end{aligned} \tag{34}$$

being a LCP.[35] This LCP (and with it the MLCP) is guaranteed to have a unique solution if all principal minors of the matrix $\left[\overline{\mathbf{M}} - \overline{\boldsymbol{\mathcal{O}}}\boldsymbol{\mathcal{O}}^{\dagger}\mathbf{M}\right]$ are strictly positive,[35] which cannot easily be checked in this general form. However, it has to be checked for a specific system at hand and serves, together with the rank condition for $\boldsymbol{\mathcal{O}}$, as a sufficient observability condition. Once $\mathbf{W}$ is known from the LCP solution, the current state is calculated with (33) and (31), that is,

$$\mathbf{x}_{n-1} = \mathbf{A}^{n-1}\boldsymbol{\mathcal{O}}^{\dagger}\mathbf{Y} + [\mathbf{Q} - \mathbf{A}^{n-1}\boldsymbol{\mathcal{O}}^{\dagger}\mathbf{M}]\mathbf{W}, \tag{35}$$

where $\mathbf{Q} := \mathbf{Q}_{n-1}$.

Remark 2. In order to obtain a state estimate at every time step k one applies (34), (35) to a moving time window of n time steps, that is,

$$\mathbf{x}_k = \mathbf{A}^{n-1}\boldsymbol{\mathcal{O}}^{\dagger}\mathbf{Y}_{k,n-1} + [\mathbf{Q} - \mathbf{A}^{n-1}\boldsymbol{\mathcal{O}}^{\dagger}\mathbf{M}]\mathbf{W}_{k,n-1}, \tag{36}$$

where $\mathbf{Y}_{k,n-1} := \left(\mathbf{y}_{k-n+1}^{\mathsf{T}} \ \dots \ \mathbf{y}_k^{\mathsf{T}}\right)^{\mathsf{T}}$ and $\mathbf{W}_{k,n-1} := \left(\mathbf{w}_{k-n+1}^{\mathsf{T}} \ \dots \ \mathbf{w}_k^{\mathsf{T}}\right)^{\mathsf{T}}$.

Remark 3. It is easy to verify that if inputs are taken into consideration, the moving window deadbeat observer reads

$$\begin{aligned}\mathbf{x}_k &= \mathbf{A}^{n-1}\boldsymbol{\mathcal{O}}^{\dagger}\mathbf{Y}_{k,n-1} + [\mathbf{Q} - \mathbf{A}^{k}\boldsymbol{\mathcal{O}}^{\dagger}\mathbf{M}]\mathbf{W}_{k,n-1} + [\mathbf{R} - \mathbf{A}^{k}\boldsymbol{\mathcal{O}}^{\dagger}\mathbf{N}]\mathbf{V}_{k,n-1},\\ \mathbf{Z}_{k,n-1} &= \left[\overline{\mathbf{M}} - \overline{\boldsymbol{\mathcal{O}}}\boldsymbol{\mathcal{O}}^{\dagger}\mathbf{M}\right]\mathbf{W}_{k,n-1} + \overline{\boldsymbol{\mathcal{O}}}\boldsymbol{\mathcal{O}}^{\dagger}\mathbf{Y}_{k,n-1} + \left[\overline{\mathbf{N}} - \overline{\boldsymbol{\mathcal{O}}}\boldsymbol{\mathcal{O}}^{\dagger}\mathbf{N}\right]\mathbf{V}_{k,n-1},\\ 0 &\leq \mathbf{Z}_{k,n-1} \perp \mathbf{W}_{k,n-1} \geq 0,\end{aligned} \tag{37}$$

where $\mathbf{V}_{k,n-1} := \left(\mathbf{v}_{k-n+1}^{\mathsf{T}} \ \dots \ \mathbf{v}_k^{\mathsf{T}}\right)^{\mathsf{T}}$ are the collected inputs, $\mathbf{R} := \left[\mathbf{A}^{k-1}\mathbf{E} \quad \mathbf{A}^{k-2}\mathbf{E} \quad \dots \quad \mathbf{E} \quad \mathbf{0}\right]$, and the two remaining matrices are

$$\mathbf{N} := \begin{bmatrix} \mathbf{0} & \mathbf{0} & \mathbf{0} & \dots & \mathbf{0} \\ \mathbf{GE} & \mathbf{0} & \mathbf{0} & \dots & \mathbf{0} \\ \mathbf{GAE} & \mathbf{GE} & \mathbf{0} & \dots & \mathbf{0} \\ \vdots & & & & \vdots \\ \mathbf{GA}^{k-1}\mathbf{E} & \mathbf{GA}^{k-2}\mathbf{E} & \dots & \mathbf{GE} & \mathbf{0} \end{bmatrix}, \quad \overline{\mathbf{N}} := \begin{bmatrix} \mathbf{F} & \mathbf{0} & \mathbf{0} & \dots & \mathbf{0} \\ \mathbf{CE} & \mathbf{F} & \mathbf{0} & \dots & \mathbf{0} \\ \mathbf{CAE} & \mathbf{CE} & \mathbf{F} & \dots & \mathbf{0} \\ \vdots & & & & \vdots \\ \mathbf{CA}^{k-1}\mathbf{E} & \mathbf{CA}^{k-2}\mathbf{E} & \dots & \mathbf{CE} & \mathbf{F} \end{bmatrix}. \tag{38}$$

5 | PASSIVITY-BASED OBSERVERS FOR DISCRETE LCS

The deadbeat approach presented in the last section suffers from one main drawback: the state estimate is highly sensitive on measurement and model errors. One reason is that the observability matrix $\boldsymbol{\mathcal{O}}$ is often ill-conditioned and, therefore, taking the (left) inverse, strongly amplifies measurement noise. Therefore an asymptotic state observer is much more desirable in practical applications. For continuous-time LCSs, Heemels et al.[37] suggest a Luenberger-type state observer, where the observer gains are determined based on a linear matrix inequality (LMI) related to system passivity. The equivalent procedure is presented here for discrete LCSs. In analogy to Reference 38, we define passivity for discrete-time systems as follows.

Definition 1. A linear time-invariant discrete-time system

$$\begin{aligned}\mathbf{x}_{k+1} &= \mathbf{A}\mathbf{x}_k + \mathbf{B}\mathbf{w}_k,\\ \mathbf{y}_k &= \mathbf{C}\mathbf{x}_k + \mathbf{D}\mathbf{w}_k,\end{aligned} \tag{39}$$

written in short as system $(\mathbf{A}, \mathbf{B}, \mathbf{C}, \mathbf{D})$, is said to be ***passive*** if there exists a nonnegative function $V : \mathbb{R}^n \to \mathbb{R}$ (called the storage function) with $V(\mathbf{0}) = 0$ such that

$$V(\mathbf{x}_{k+1}) - V(\mathbf{x}_k) \leq \mathbf{y}_k^\mathsf{T} \mathbf{w}_k \tag{40}$$

$\forall\, \mathbf{w}_k$ and $\forall\, k$.

A useful result with respect to passivity, adapted from Reference 39 to discrete-time systems, is the following theorem, in which we use the notation $\mathbf{M} \leq 0$ and $\mathbf{M} < 0$ to express that a matrix $\mathbf{M}$ is negative semidefinite and negative definite, respectively. Likewise, $\mathbf{M} \geq 0$ and $\mathbf{M} > 0$ express positive semidefiniteness and positive definiteness of $\mathbf{M}$.

Theorem 1. System (39) is passive if and only if there exists a matrix $\mathbf{P} = \mathbf{P}^\mathsf{T} \geq 0$ such that the following matrix inequality holds

$$\begin{pmatrix} \mathbf{A}^\mathsf{T}\mathbf{P}\mathbf{A} - \mathbf{P} & \mathbf{A}^\mathsf{T}\mathbf{P}\mathbf{B} - \mathbf{C}^\mathsf{T} \\ \mathbf{B}^\mathsf{T}\mathbf{P}\mathbf{A} - \mathbf{C} & \mathbf{B}^\mathsf{T}\mathbf{P}\mathbf{B} - (\mathbf{D} + \mathbf{D}^\mathsf{T}) \end{pmatrix} \leq 0. \tag{41}$$

In analogy to Reference 37, we define the slightly stronger property, known as strict passivity, as follows.

Definition 2. System (39) is said to be ***strictly passive*** if there exists a matrix $\mathbf{P} = \mathbf{P}^\mathsf{T} > 0$ and a constant $\mu > 0$ such that the matrix inequality

$$\begin{pmatrix} \mathbf{A}^\mathsf{T}\mathbf{P}\mathbf{A} - \mathbf{P} + \mu\mathbf{P} & \mathbf{A}^\mathsf{T}\mathbf{P}\mathbf{B} - \mathbf{C}^\mathsf{T} \\ \mathbf{B}^\mathsf{T}\mathbf{P}\mathbf{A} - \mathbf{C} & \mathbf{B}^\mathsf{T}\mathbf{P}\mathbf{B} - (\mathbf{D} + \mathbf{D}^\mathsf{T}) \end{pmatrix} \leq 0 \tag{42}$$

holds.

Note that if the system (39) is strictly passive, then the inequality (40) holds strictly. Now consider a general discrete LCS (not necessarily the discretization of the dynamics of a mechanical system) of the form (25). The proposed Luenberger-type state observer for the discrete LCS (25) is in analogy to Reference 37

$$\begin{aligned} \hat{\mathbf{x}}_{k+1} &= \mathbf{A}\hat{\mathbf{x}}_k + \mathbf{B}\hat{\mathbf{w}}_k + \mathbf{E}\mathbf{v}_k + \mathbf{L}_1(\mathbf{y}_k - \hat{\mathbf{y}}_k), \\ \hat{\mathbf{z}}_k &= \mathbf{C}\hat{\mathbf{x}}_k + \mathbf{D}\hat{\mathbf{w}}_k + \mathbf{F}\mathbf{v}_k + \mathbf{L}_2(\mathbf{y}_k - \hat{\mathbf{y}}_k), \\ 0 &\leq \hat{\mathbf{z}}_k \perp \hat{\mathbf{w}}_k \geq 0, \\ \hat{\mathbf{y}}_k &= \mathbf{G}\hat{\mathbf{x}}_k, \end{aligned} \tag{43}$$

where all observer related quantities are written with a circumflex ($\hat{}$). The observer consists of a copy of the original system, augmented by two correction terms, both linear in the output difference. Defining the observation errors as $\tilde{\mathbf{x}}_k := \mathbf{x}_k - \hat{\mathbf{x}}_k$, $\tilde{\mathbf{z}}_k := \mathbf{z}_k - \hat{\mathbf{z}}_k$ and $\tilde{\mathbf{w}}_k := \mathbf{w}_k - \hat{\mathbf{w}}_k$, it follows that

$$\begin{aligned} \tilde{\mathbf{x}}_{k+1} &= (\mathbf{A} - \mathbf{L}_1\mathbf{G})\tilde{\mathbf{x}}_k + \mathbf{B}\tilde{\mathbf{w}}_k, \\ \tilde{\mathbf{z}}_k &= (\mathbf{C} - \mathbf{L}_2\mathbf{G})\tilde{\mathbf{x}}_k + \mathbf{D}\tilde{\mathbf{w}}_k, \\ \tilde{\mathbf{z}}_k^\mathsf{T}\tilde{\mathbf{w}}_k &\leq 0. \end{aligned} \tag{44}$$

The last relation in (44) is easily checked by expanding

$$\tilde{\mathbf{z}}_k^\mathsf{T}\tilde{\mathbf{w}}_k = (\mathbf{z}_k - \hat{\mathbf{z}}_k)^\mathsf{T}(\mathbf{w}_k - \hat{\mathbf{w}}_k) = \mathbf{z}_k^\mathsf{T}\mathbf{w}_k - \mathbf{z}_k^\mathsf{T}\hat{\mathbf{w}}_k - \hat{\mathbf{z}}_k^\mathsf{T}\mathbf{w}_k + \hat{\mathbf{z}}_k^\mathsf{T}\hat{\mathbf{w}}_k. \tag{45}$$

Therein, the first and the last term vanish and the two other terms are non-positive due to the inequality complementarities in (25) and (43). Note that the inequality $\tilde{\mathbf{z}}_k^\mathsf{T}\tilde{\mathbf{w}}_k \leq 0$ represents the monotonicity property of the discrete impact law for mechanical systems. It is however not an inequality complementarity. Equation (44) does therefore not form a full description of the error dynamics, because $\tilde{\mathbf{w}}_k$ cannot be expressed as a function of the estimation error $\tilde{\mathbf{x}}_k$. We rather have to use the last three lines of (25) and (43). As a consequence, $\tilde{\mathbf{w}}_k$ depends on $\mathbf{x}_k$, $\hat{\mathbf{x}}_k$, and $\mathbf{v}_k$, where $\hat{\mathbf{x}}_k$ can be replaced

by $\mathbf{x}_k - \tilde{\mathbf{x}}_k$ (or the other way around). As pointed out in Reference 37 for the continuous-time case, the error dynamics is therefore nonautonomous and has two states, $\tilde{\mathbf{x}}_k$ and $\mathbf{x}_k$ (or alternatively $\tilde{\mathbf{x}}_k$ and $\hat{\mathbf{x}}_k$). However, only the estimation error $\tilde{\mathbf{x}}_k$ has to tend to zero as k increases. It is worth mentioning that in (44), $\tilde{\mathbf{w}}_k$ is not seen as a disturbance on the error dynamics, as in the case of a unilaterally constrained mechanical system, it represents the error in the constraint forces which constitute a fundamental aspect of the dynamics. From the inequality in (44), it follows that if system $(\mathbf{A} - \mathbf{L}_1\mathbf{G}, \mathbf{B}, \mathbf{C} - \mathbf{L}_2\mathbf{G}, \mathbf{D})$ is strictly passive, the corresponding storage function serves as a Lyapunov function to show asymptotic stability of the estimation error. Indeed, we can select $V(\tilde{\mathbf{x}}_k) = \tilde{\mathbf{x}}_k^\mathsf{T}\mathbf{P}\tilde{\mathbf{x}}_k$ with $\mathbf{P} = \mathbf{P}^\mathsf{T} > 0$ and calculate

$$\begin{aligned} V(\tilde{\mathbf{x}}_{k+1}) - V(\tilde{\mathbf{x}}_k) &= \tilde{\mathbf{x}}_{k+1}^\mathsf{T}\mathbf{P}\tilde{\mathbf{x}}_{k+1} - \tilde{\mathbf{x}}_k^\mathsf{T}\mathbf{P}\tilde{\mathbf{x}}_k \\ &= (\tilde{\mathbf{x}}_{k+1} + \tilde{\mathbf{x}}_k)^\mathsf{T}\mathbf{P}(\tilde{\mathbf{x}}_{k+1} - \tilde{\mathbf{x}}_k) \\ &= ((\mathbf{A} - \mathbf{L}_1\mathbf{G})\tilde{\mathbf{x}}_k + \mathbf{B}\tilde{\mathbf{w}}_k + \tilde{\mathbf{x}}_k)^\mathsf{T}\mathbf{P}((\mathbf{A} - \mathbf{L}_1\mathbf{G})\tilde{\mathbf{x}}_k + \mathbf{B}\tilde{\mathbf{w}}_k - \tilde{\mathbf{x}}_k), \end{aligned} \tag{46}$$

which, after first subtracting and then again adding the term $2\tilde{\mathbf{z}}_k^\mathsf{T}\tilde{\mathbf{w}}_k$, can be written as

$$\begin{aligned} V(\tilde{\mathbf{x}}_{k+1}) - V(\tilde{\mathbf{x}}_k) = &\begin{pmatrix} \tilde{\mathbf{x}}_k \\ \tilde{\mathbf{w}}_k \end{pmatrix}^\mathsf{T} \begin{pmatrix} (\mathbf{A} - \mathbf{L}_1\mathbf{G})^\mathsf{T}\mathbf{P}(\mathbf{A} - \mathbf{L}_1\mathbf{G}) - \mathbf{P} & (\mathbf{A} - \mathbf{L}_1\mathbf{G})^\mathsf{T}\mathbf{P}\mathbf{B} - (\mathbf{C} - \mathbf{L}_2\mathbf{G})^\mathsf{T} \\ \mathbf{B}^\mathsf{T}\mathbf{P}(\mathbf{A} - \mathbf{L}_1\mathbf{G}) - (\mathbf{C} - \mathbf{L}_2\mathbf{G}) & \mathbf{B}^\mathsf{T}\mathbf{P}\mathbf{B} - (\mathbf{D} + \mathbf{D}^\mathsf{T}) \end{pmatrix} \begin{pmatrix} \tilde{\mathbf{x}}_k \\ \tilde{\mathbf{w}}_k \end{pmatrix} \\ &+ 2\tilde{\mathbf{z}}_k^\mathsf{T}\tilde{\mathbf{w}}_k. \end{aligned} \tag{47}$$

Because $\tilde{\mathbf{z}}_k^\mathsf{T}\tilde{\mathbf{w}}_k \leq 0$, it follows that if the system $(\mathbf{A} - \mathbf{L}_1\mathbf{G}, \mathbf{B}, \mathbf{C} - \mathbf{L}_2\mathbf{G}, \mathbf{D})$ is strictly passive, we have $V(\tilde{\mathbf{x}}_{k+1}) - V(\tilde{\mathbf{x}}_k) \leq -\mu V(\tilde{\mathbf{x}}_k)$. In that case, the estimation error dynamics is asymptotically stable. The matrix inequality

$$\begin{pmatrix} (\mathbf{A} - \mathbf{L}_1\mathbf{G})^\mathsf{T}\mathbf{P}(\mathbf{A} - \mathbf{L}_1\mathbf{G}) - \mathbf{P} + \mu\mathbf{P} & (\mathbf{A} - \mathbf{L}_1\mathbf{G})^\mathsf{T}\mathbf{P}\mathbf{B} - (\mathbf{C} - \mathbf{L}_2\mathbf{G})^\mathsf{T} \\ \mathbf{B}^\mathsf{T}\mathbf{P}(\mathbf{A} - \mathbf{L}_1\mathbf{G}) - (\mathbf{C} - \mathbf{L}_2\mathbf{G}) & \mathbf{B}^\mathsf{T}\mathbf{P}\mathbf{B} - (\mathbf{D} + \mathbf{D}^\mathsf{T}) \end{pmatrix} \leq 0, \tag{48}$$

that we need to fulfill to ensure strict passivity, is nonlinear in the unknowns $\mathbf{L}_1, \mathbf{L}_2$ and $\mathbf{P}$. However, by introducing $\mathbf{S} := \mathbf{P}\mathbf{L}_1$ and applying the Schur complement lemma, it can be checked that (48) is equivalent to the LMI

$$\begin{pmatrix} -\mathbf{P} + \mu\mathbf{P} & -(\mathbf{C} - \mathbf{L}_2\mathbf{G})^\mathsf{T} & \mathbf{A}^\mathsf{T}\mathbf{P} - \mathbf{G}^\mathsf{T}\mathbf{S}^\mathsf{T} \\ -(\mathbf{C} - \mathbf{L}_2\mathbf{G}) & -(\mathbf{D} + \mathbf{D}^\mathsf{T}) & \mathbf{B}^\mathsf{T}\mathbf{P} \\ \mathbf{P}\mathbf{A} - \mathbf{S}\mathbf{G} & \mathbf{P}\mathbf{B} & -\mathbf{P} \end{pmatrix} \leq 0. \tag{49}$$

Since $\mathbf{P}$ is invertible, $\mathbf{L}_1$ can be recovered in a second step as $\mathbf{L}_1 = \mathbf{P}^{-1}\mathbf{S}$. The transformation from the nonlinear matrix inequality (48) to the LMI (49) is very useful, since efficient numerical LMI solvers are available. Note however that imposing additional constraints on the solutions of (49) can lead again to a nonlinear matrix inequality. For example, if one wants to introduce the constraint $\mathbf{L}_2 = \mathbf{T}\mathbf{L}_1$ with some given matrix $\mathbf{T}$, one would need to be replace $\mathbf{L}_2 = \mathbf{T}\mathbf{L}_1 = \mathbf{T}\mathbf{P}^{-1}\mathbf{S}$ in (49), rendering the matrix inequality again nonlinear.

5.1 | An extended version for position measurements

In our case of a mechanical system, $\mathbf{z}_k$ represents the kinematic variable $\boldsymbol{\zeta}_k = \mathbf{g}_{k+1} + \varepsilon\mathbf{g}_{k-1}$ in (16). Therefore $\mathbf{z}_k$, and with it $\tilde{\mathbf{z}}_k$, depend on one past value $\mathbf{g}_{k-1}$ of the contact distance and one future value $\mathbf{g}_{k+1}$. It therefore makes sense to extended the observer (43) to include past and future measurements at t_{k-1} and t_{k+1}, respectively. We add more correction terms as follows

$$\begin{aligned} \hat{\mathbf{x}}_{k+1} &= \mathbf{A}\hat{\mathbf{x}}_k + \mathbf{B}\hat{\mathbf{w}}_k + \mathbf{E}\mathbf{v}_k + \mathbf{L}_1(\mathbf{y}_k - \hat{\mathbf{y}}_k) + \mathbf{L}_3\left(\mathbf{y}_{k+1} - \hat{\mathbf{y}}_{k+1}^{(-)}\right) + \mathbf{L}_5\left(\mathbf{y}_{k-1} - \hat{\mathbf{y}}_{k-1}^{(-)}\right), \\ \hat{\mathbf{z}}_k &= \mathbf{C}\hat{\mathbf{x}}_k + \mathbf{D}\hat{\mathbf{w}}_k + \mathbf{F}\mathbf{v}_k + \mathbf{L}_2(\mathbf{y}_k - \hat{\mathbf{y}}_k) + \mathbf{L}_4\left(\mathbf{y}_{k+1} - \hat{\mathbf{y}}_{k+1}^{(-)}\right) + \mathbf{L}_6\left(\mathbf{y}_{k-1} - \hat{\mathbf{y}}_{k-1}^{(-)}\right), \\ 0 &\leq \hat{\mathbf{z}}_k \perp \hat{\mathbf{w}}_k \geq 0, \\ \hat{\mathbf{y}}_k &= \mathbf{G}\hat{\mathbf{x}}_k, \end{aligned} \tag{50}$$

where $\hat{\mathbf{y}}_{k+1}^{(-)} := \mathbf{G}(\mathbf{A}\hat{\mathbf{x}}_k + \mathbf{B}\hat{\mathbf{w}}_k + \mathbf{E}\mathbf{v}_k)$ is the predicted future output without considering the correction terms. Similarly, $\mathbf{y}_{k-1}^{(-)}$ refers to the past output, obtained by back-propagation without considering correction terms. As we did in (22), we can back-propagate positions with the kinematic equation $\mathbf{q}_{k-1} = \mathbf{q}_k - \Delta t \mathbf{u}_k$. Here, we restrict ourselves to the case where the output $\mathbf{y}_k$ depends only on positions $\mathbf{q}_k$. The reason for this is that obtaining past velocities $\mathbf{u}_{k-1}$ by back-propagation would involve past values $\mathbf{w}_{k-1}$ and $\mathbf{v}_{k-1}$, such that the estimation error dynamics would become structurally different from (44). In addition, in cases where $\mathbf{A}$ is not invertible, the back-propagation might not have a (unique) solution. We will write $\mathbf{y}_{k-1} = \mathbf{G}\mathbf{x}_{k-1} = \mathbf{G}\tilde{\mathbf{A}}\mathbf{x}_k$ with the back-propagation matrix $\tilde{\mathbf{A}} := (\mathbf{I} \ -\Delta t\mathbf{I}; \mathbf{0} \ \ \mathbf{0})$, where $\mathbf{I}$ is a unit matrix of appropriate dimensions and a semicolon is used to separate rows. With $\tilde{\mathbf{x}}_{k+1} = \mathbf{x}_{k+1} - \mathbf{x}_k$ the error dynamics can be written as

$$\begin{aligned}
\tilde{\mathbf{x}}_{k+1} &= (\mathbf{A} - \mathbf{L}_1\mathbf{G} - \mathbf{L}_3\mathbf{G}\mathbf{A} - \mathbf{L}_5\mathbf{G}\tilde{\mathbf{A}})\tilde{\mathbf{x}}_k + (\mathbf{B} - \mathbf{L}_3\mathbf{G}\mathbf{B})\tilde{\mathbf{w}}_k,\\
\tilde{\mathbf{z}}_k &= (\mathbf{C} - \mathbf{L}_2\mathbf{G} - \mathbf{L}_4\mathbf{G}\mathbf{A} - \mathbf{L}_6\mathbf{G}\tilde{\mathbf{A}})\tilde{\mathbf{x}}_k + (\mathbf{D} - \mathbf{L}_4\mathbf{G}\mathbf{B})\tilde{\mathbf{w}}_k,\\
\tilde{\mathbf{z}}_k^{\mathrm{T}}\tilde{\mathbf{w}}_k &\le 0,
\end{aligned} \tag{51}$$

which is of the same form as (44) but with more design variables. Therefore, we can follow the same steps as in (46) to (49) to obtain a LMI.

Remark 4. The observer dynamics (50) can alternatively be written as

$$\begin{aligned}
\hat{\mathbf{x}}_{k+1} &= (\mathbf{A} - \mathbf{L}_1\mathbf{G} - \mathbf{L}_3\mathbf{G}\mathbf{A} - \mathbf{L}_5\mathbf{G}\tilde{\mathbf{A}})\hat{\mathbf{x}}_k + (\mathbf{B} - \mathbf{L}_3\mathbf{G}\mathbf{B})\hat{\mathbf{w}}_k + (\mathbf{E} - \mathbf{L}_3\mathbf{G}\mathbf{E})\mathbf{v}_k\\
&\quad + \mathbf{L}_1\mathbf{y}_k + \mathbf{L}_3\mathbf{y}_{k+1} + \mathbf{L}_5\mathbf{y}_{k-1},\\
\hat{\mathbf{z}}_k &= (\mathbf{C} - \mathbf{L}_2\mathbf{G} - \mathbf{L}_4\mathbf{G}\mathbf{A} - \mathbf{L}_6\mathbf{G}\tilde{\mathbf{A}})\hat{\mathbf{x}}_k + (\mathbf{D} - \mathbf{L}_4\mathbf{G}\mathbf{B})\hat{\mathbf{w}}_k + (\mathbf{F} - \mathbf{L}_4\mathbf{G}\mathbf{E})\mathbf{v}_k\\
&\quad + \mathbf{L}_2\mathbf{y}_k + \mathbf{L}_4\mathbf{y}_{k+1} + \mathbf{L}_6\mathbf{y}_{k-1},\\
0 &\le \hat{\mathbf{z}}_k \perp \hat{\mathbf{w}}_k \ge 0.
\end{aligned} \tag{52}$$

To ensure the existence of a unique solution, the observer gain $\mathbf{L}_4$ has therefore to be designed such that $\mathbf{D} - \mathbf{L}_4\mathbf{G}\mathbf{B}$ is a $\mathcal{P}$-matrix.

Remark 5. If $\mathbf{L}_3$ can be designed such that $\mathbf{B} - \mathbf{L}_3\mathbf{G}\mathbf{B} = \mathbf{0}$, the state error in (51) becomes independent of $\tilde{\mathbf{w}}_k$. We are then left with designing $\mathbf{L}_1$ and $\mathbf{L}_5$ such that the error dynamics is asymptotically stable. This corresponds to an *unknown input observer* as it is known for linear systems. However, as in our numerical example below, such a gain $\mathbf{L}_3$ often does not exist.

6 | NUMERICAL EXAMPLE

As an example system, consider the two-mass oscillator depicted in Figure 1. The oscillator with masses m, spring constants k and damping ratios d is excited by an external force $F(t)$ applied to the first mass and the movement of the second mass is restricted by a motion limiting stop. The positions of the two masses, relative to the equilibrium positions for $F = 0$, are described by the coordinates q_1 and q_2 . The system dynamics is described by (7) with

$$\mathbf{M} = \begin{pmatrix} m & 0 \\ 0 & m \end{pmatrix}, \mathbf{K} = \begin{pmatrix} 2k & -k \\ -k & k \end{pmatrix}, \mathbf{D} = \begin{pmatrix} 2d & -d \\ -d & d \end{pmatrix}, \mathbf{W} = \begin{pmatrix} 0 \\ -1 \end{pmatrix}, \text{ and } \mathbf{f} = \begin{pmatrix} 1 \\ 0 \end{pmatrix} F(t). \tag{53}$$

The parameters are given by $m = 1$ kg, $k = 1500$ N/m, $d = 0.5$ N s/m, and the coefficient of restitution is $\varepsilon = 0.8$. We use a periodic excitation $F(t) = a\sin(\omega t)$ with an amplitude of $a = 10$ N and a frequency $\omega = 5.25 \cdot 2\pi$ rad/s.

To reduce large differences in the order of magnitude of numerical values during the solution, we scale $\mathbf{u}_k$ and $\mathbf{w}_k$ by the time step length Δt prior to solving the LMI. More precisely, in (25), we replace the velocity $\mathbf{u}_k$ by $\Delta\mathbf{q}_k := \mathbf{q}_k - \mathbf{q}_{k-1}$ and $\mathbf{w}_k$ by $\Delta t\overline{\mathbf{w}}_k$. As a result, we obtain scaled system matrix entries (which are not given here). The LMI (49) and its extended counterpart are then solved with the scaled system matrices using the Matlab integrated LMI solver *feasp*, which is based on a projective method.[40] In the following, we will have a closer look at three cases of different difficulty:

- Case I with output $\mathbf{y}_k = \mathbf{q}_k$, that is, all positions are measured with $\mathbf{G} = \begin{pmatrix} 1 & 0 & 0 & 0 \\ 0 & 1 & 0 & 0 \end{pmatrix}$

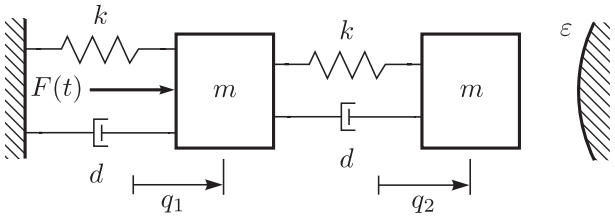

FIGURE 1 An example system with one unilateral constraint.

- Case II with output $\mathbf{y}_k = q_{1k}$, that is, only the position of the non-colliding mass is measured with $\mathbf{G} = \begin{pmatrix} 1 & 0 & 0 & 0 \end{pmatrix}$
- Case III with $\mathbf{y}_k = q_{2k} - q_{1k}$, that is, the difference between the two mass positions are measured with $\mathbf{G} = \begin{pmatrix} -1 & 1 & 0 & 0 \end{pmatrix}$

Even though in all three cases positions are measured, these cases are different in their difficulty because they do not fulfill the same observability conditions. Case I is the easiest, since we directly know from measurements whether or not the contact is open or closed. As mentioned in the introduction, in that case several existing observer designs are applicable. The observability matrix $\boldsymbol{\mathcal{O}}$ has full column rank in all three cases, indicating that the non-impulsive dynamics is observable in all cases. For the (discretized) impulsive dynamics, we introduced a sufficient observability condition in Section 4: if the matrix $\left[\overline{\mathbf{M}} - \overline{\boldsymbol{\mathcal{O}}}\boldsymbol{\mathcal{O}}^{+}\mathbf{M}\right]$ is a $\mathcal{P}$ -matrix, then the LCP (34) has a unique solution. This observability condition is fulfilled in case I and case II, but not in case III. Therefore, for the cases I and II, observability is confirmed and the deadbeat observer (34), (35) is applicable, while for case III observability remains undetermined and the deadbeat observer is not applicable. Regarding the passivity-based observers from Section 5, for case I both, the LMI (49) and its extended counterpart, admit a solution. For case II, only the LMI of the extended observer version admits a solution, which shows the necessity to include past and future measurements in the observer in the presence of unilateral constraints. Finally, for case III, both LMIs do not admit a solution. Therefore, the passivity-based observer is not applicable in case III which we will exclude from further discussion. In the following we will concentrate our discussion on case II, since it was observed in the numerical analysis that case I shows a similar behavior, but case II is more difficult and therefore more interesting. The first thing we observe from the numerical LMI solution of case II is that the entries of the observer gains $\mathbf{L}_i$ $(i = 1, \dots, 6)$ increase as the step size Δt decreases. Figure 2 shows the maximum absolute value of all observer gain entries as a function of Δt^2 . The observer gains are roughly inversely proportional to the squared time step size. As a result of the high observer gains for small time steps, the initial observer error is often strongly amplified at the beginning. In Figure 3, the trajectories of the impacting mass are plotted for both, the discretization of the observed system and the corresponding extended passivity-based observer, with $\Delta t = 10^{-4}$ s and selected initial conditions. The velocity estimation strongly deviates from the true trajectory for a short period of time. This phenomenon is also known as "peaking" in the literature on high-gain observers,[41] but is not to be confused with the peaking phenomenon of impulsive systems, which refers to the fact that the Euclidean error between trajectories can jump to high values, even if the trajectories are arbitrarily close. The Lyapunov function (and with it the state estimation error), however, decreases quickly, as shown in Figure 4. A real-time implementation of the state observer is challenging for very small time steps. In our numerical example, the average computation time per time step on a standard desktop PC is $2.5 \cdot 10^{-5}$ s. Here, we chose $\Delta t = 10^{-4}$ s for presentation. For other time steps Δt , the qualitative behavior of the extended passivity-based observer is similar, with higher deflections in the transient phase for lower Δt .

Large entries in the observer gains $\mathbf{L}_i$ $(i = 1, \dots, 6)$ have a negative influence on the observer's robustness against measurement noise, since in the observer dynamics (52), they are multiplied by the measurements. Because the observer gain entries are roughly inversely proportional to the squared step size Δt^2, one might therefore be tempted to select a large step size. However, a large time step would cause a pronounced deviation between the continuous-time system and the discrete-time model. Furthermore, the ability of the time discretization to describe collisions which are separated by a short period of time also depends on the chosen time step. Compared to the observer design for linear systems, where the designer is usually facing a performance-robustness tradeoff when selecting the observer gains, the situation is more complicated here. For each system at hand, the observer's sensitivity to variations in the step size has to be analyzed and it has to be decided, if a certain step size leads to admissible noise levels.

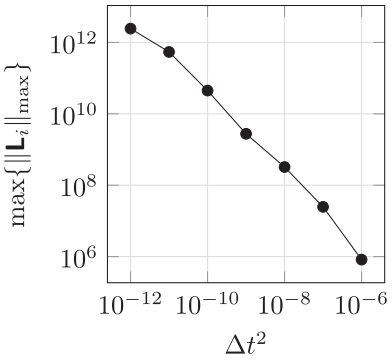

FIGURE 2 Case II: Logarithmic plot of the maximum observer gain entry $\max\{\|\mathbf{L}_i\|_{\max}\}$ $(i = 1, \dots, 6)$ as a function of the squared step size Δt^2 (in s^2). Here $\|\mathbf{L}_i\|_{\max} := \max_{i,j} |\ell_{ij}|$ if ℓ_{ij} are the scalar entries of $\mathbf{L}_i$.

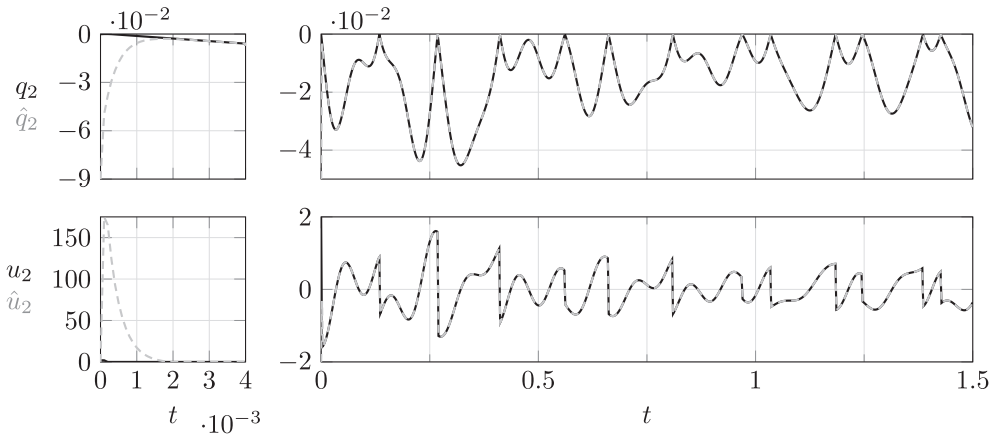

FIGURE 3 Example case II with $\Delta t = 10^{-4}$ s and the initial conditions $\mathbf{x}_0 = (0, -10^{-4}, 1, 2)$ and $\hat{\mathbf{x}}_0 = (0, -10^{-1}, 10^{-4}, 10^{-4})$ (in m and m/s resp.). Trajectories of the impacting mass (solid black: observed system (discretized), dashed gray: extended observer) over 10 periods of excitation (t in s, q_2 in m, u_2 in m/s). On the left, the transient phase is shown with a different zoom: The extended observer strongly deviates from the true trajectory in the beginning, due to the large observer gains.

Interestingly, in our example, measurement noise has a marginal influence on the observer's impact law, compared to the strong influence on the non-impulsive motion due to the high observer gains. In Figure 5, the first two plots show the true and estimated velocities u_2 and $\hat{u}_2$ for the extended observer with additive, normally distributed noise on the measurements. More precisely, we use $y_k = \mathbf{G}\mathbf{x}_k + d_k$ with $d_k \sim \mathcal{N}(0, \sigma^2)$, that is, d_k is a discrete random variable drawn from a normal distribution with zero mean and standard deviation σ. It is observed, that even small standard deviations lead to strong noise levels on the velocity estimation $\hat{u}_2$. The step height during the impulsive motion however is only marginally altered by the measurement noise, as is shown in the zoom plots on the right-hand side of Figure 5. Conversely, a time step Δt which is long compared to the actual contact duration, mainly affects the step height of the observer during the impulsive motion, whereas the non-impulsive motion is only marginally altered. This is shown in the last plot of Figure 5. Therein, the true trajectory is generated by simulating an LCS with a time step Δt_{sim} which is an order of magnitude smaller than the time step Δt used for the observer design. From the zoom on the right-hand side, it can be observed that due to the difference in the time steps, the observer's step height during the impulsive motion is smaller than the actual step height.

It is worth mentioning that the chosen time step does not have an immediate effect on the impact law of the discrete-time model. Furthermore, without measurement noise and modeling errors, the impact law of the passivity-based state observer is identical to the impact law of the discretized observed system after the estimation error converged to zero. However, before the estimation error converged to zero (i.e., if the output of the observer is not identical to the measurements), the observer's impact law is not physical and the correction terms in the observer dynamics have an influence on how the contact velocity changes during phases of contact. In other words, the chosen time step does have an effect on the observer's impact law, but since this impact law is not physical, this does not impose any constraints on the time step.

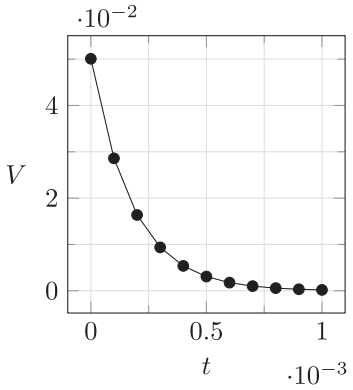

FIGURE 4 Lyapunov function $V(\tilde{\mathbf{x}}_k) = \tilde{\mathbf{x}}_k^\mathsf{T}\mathbf{P}\tilde{\mathbf{x}}_k$ over time t (in s) for the example in Figure 3.

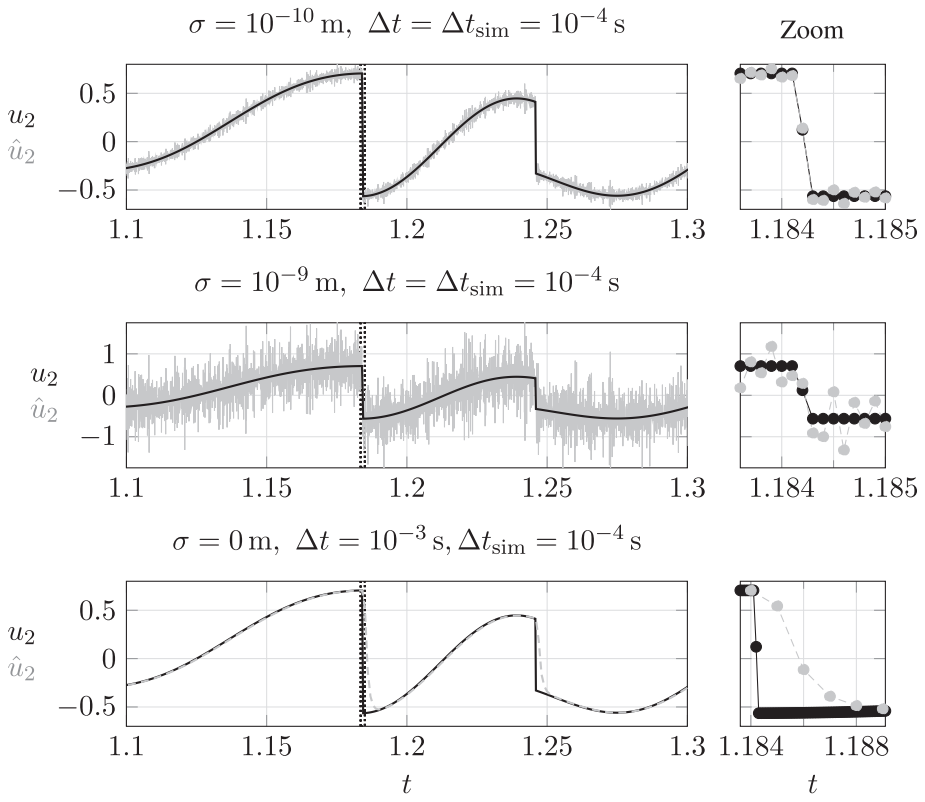

FIGURE 5 Influence of measurement noise and a time step error on the velocity estimation $\hat{u}_2$ of the impacting mass for case II (initial conditions identical to Figure 3). Solid black: Observed system (discretized), gray: extended observer (u_2 in m/s, t in s). The first plot shows the influence of a normally distributed measurement noise with zero mean and a standard deviation $\sigma = 10^{-10}$ m. In the second plot, the standard deviation is 10^{-9} m. In the third plot, the true trajectory is generated by simulating the LCS with Δt_{sim} which is smaller than Δt of the observer.

7 | CONCLUSION

In this work, we have tried to give the research on developing an observer design for unilaterally constrained mechanical systems *without* using contact measurement a new impulse. As this article shows again, this remains a difficult task. We summarize the steps we have taken and try to identify the merits of the article.

The first important step has been to consider a discrete approximation of the original continuous-time system. We have shown that the deliberate choice of the Schatzman–Paoli scheme leads to a discrete LCS (whereas other

schemes do not). This can be seen as a result of the article, which may also be useful outside the scope of observer design.

The formulation as discrete LCS opens the way for the derivation of a deadbeat observer for this type of systems. We have shown that a deadbeat observer for a discrete LCS leads to a mixed LCP. In addition, we obtained a sufficient observability condition, by requiring that the mixed LCP has a unique solution. The deadbeat observer, however, is not robust with respect to measurement noise, but may serve as starting point for future research.

Furthermore, the formulation as discrete LCS allows us to use existing observer design techniques for LCS as developed by Heemels et al.[37] Hereto, we have transported the existing results for continuous-time LCS to discrete LCS. The observer consists of a copy of the observed system, augmented by Luenberger-type correction terms. Here, we consider the observed system and the observer both to be discrete-time systems with matching time steps. It turns out, that the observer gains which follow from a LMI are inversely proportional to the squared time step Δt^2.

Because a small Δt leads to high observer gains, lowering the time step increases the sensitivity with respect to measurement noise. Conversely, as we are using a discrete version of the continuous time problem, increasing the time step yields a larger modeling error, since the discretization is an approximation. Compared to the performance-robustness tradeoff encountered in many other observer designs, the selection of the time step here is more complicated. For every system at hand it has to be checked if an admissible choice of the step size can lead to an acceptable performance.

Although we did not find an inherently robust observer design, we come to a fundamental insight: The discretization using the Schatzman–Paoli scheme can be viewed as a regularization which reveals that the peaking phenomenon of impulsive mechanical systems is in fact a singularity with respect to the time step Δt.

Lastly, we conclude that the body of methods we have presented here links, somewhat unexpectedly, different research topics: measure differential inclusions, mixed LCPs and LCSs. The Schatzman–Paoli scheme plays a crucial role in establishing these links.

CONFLICT OF INTEREST

All authors declare that they have no conflict of interest.

DATA AVAILABILITY STATEMENT

Data sharing is not applicable as no dataset was generated in the current study.

ORCID

Pascal V. Preiswerk https://orcid.org/0000-0003-1465-4307
Remco I. Leine https://orcid.org/0000-0001-9859-7519

REFERENCES

1. Tanwani A, Brogliato B, Prieur C. Observer design for unilaterally constrained Lagrangian systems: a passivity-based approach. *IEEE Trans Autom Control*. 2016;61(9):2386-2401.
2. Menini L, Tornambè A. Velocity observers for linear mechanical systems subject to single non-smooth impacts. *Syst Control Lett*. 2001;43(3):193-202.
3. Menini L, Tornambè A. Velocity observers for non-linear mechanical systems subject to non-smooth impacts. *Automatica*. 2002;38(12):2169-2175.
4. Baumann M, Leine RI. A synchronization-based state observer for impact oscillators using only collision time information. *Int J Robust Nonlinear Control*. 2016;26(12):2542-2563.
5. Kim J, Cho H, Shamsuarov A, Shim H, Seo JH. State estimation strategy without jump detection for hybrid systems using gluing function. Proceedings of the 53rd IEEE Conference on Decision and Control; 2014:139-144; IEEE.
6. Menini L, Tornambè A. State immersion observers for mechanical systems with impacts. Proceedings of the 2016 IEEE 55th Conference on Decision and Control (CDC); 2016:7117-7122; IEEE.
7. Biemond JJB, van de Wouw N, Heemels WPMH, Nijmeijer H. Tracking control for hybrid systems with state-triggered jumps. *IEEE Trans Automat Contr*. 2013;58(4):876-890.
8. Biemond JJB, Heemels WPMH, Sanfelice RG, van de Wouw N. Distance function design and Lyapunov techniques for the stability of hybrid trajectories. *Automatica*. 2016;73:38-46.
9. Leine RI, van de Wouw N. *Stability and Convergence of Mechanical Systems with Unilateral Constraints*. Lecture Notes in Applied and Computational Mechanics. Springer; 2008.
10. Sanfelice RG, Biemond JJB, van de Wouw N, Heemels WPMH. An embedding approach for the design of state-feedback tracking controllers for references with jumps. *Int J Robust Nonlinear Control*. 2014;24(11):1585-1608.
11. Biemond JJB, Postoyan R, Heemels WPMH, van de Wouw N. Incremental stability of hybrid dynamical systems. *IEEE Trans Automat Contr*. 2018;63(12):4094-4109.

12. Baumann M, Biemond JJB, Leine RI, van de Wouw N. Synchronization of impacting mechanical systems with a single constraint. *Phys D Nonlinear Phenomena*. 2018;362:9-23.
13. Glocker C. Energetic consistency conditions for standard impacts. Part I: Newton-type inequality impact laws and Kane's example. *Multibody Syst Dyn*. 2013;29(1):77-117.
14. Glocker C. Energetic consistency conditions for standard impacts. Part II: Poisson-type inequality impact laws. *Multibody Syst Dyn*. 2013;32(4):1-65.
15. Brogliato B. *Nonsmooth Mechanics. Models, Dynamics and Control*. Communications and Control Engineering. 3rd ed. Springer-Verlag, International Publishing; 2016.
16. Glocker C. On frictionless impact models in rigid-body systems. *Philos Trans R Soc Lond A*. 2001;359:2385-2404.
17. Winandy T, Baumann M, Leine RI. Variational analysis of inequality impact laws for perfect unilateral constraints. In: Leine RI, Acary V, Brüls O, eds. *Advanced Topics in Nonsmooth Dynamics: Transactions of the European Network for Nonsmooth Dynamics*. Springer International Publishing; 2018:47-92.
18. Moreau JJ. Unilateral contact and dry friction in finite freedom dynamics. *Non-Smooth Mechanics and Applications*. Springer-Verlag; 1988:1-82.
19. Acary V, Brogliato B. *Numerical Methods for Nonsmooth Dynamical Systems; Applications in Mechanics and Electronics*. Lecture Notes in Applied and Computational Mechanics. Vol 35. Springer-Verlag; 2008.
20. Moreau JJ. Some numerical methods in multibody dynamics: application to granular materials. *Eur J Mech A-Solids*. 1994;13:93-114.
21. Acary V, Jean M. Numerical modeling of three dimensional divided structures by the non smooth contact dynamics method: application to masonry structures. In: Topping BHV, ed. *Computational Mechanics: Techniques and Developments*. Civil-Comp Press; 2000:211-221.
22. Transeth AA, Leine RI, Glocker C, Pettersen KY. 3-D snake robot motion: nonsmooth modeling, simulations, and experiments. *IEEE Trans Robot*. 2008;24(2):361-376.
23. Paoli L, Schatzman M. A numerical scheme for impact problems I: the one-dimensional case. *SIAM J Numer Anal*. 2002;40(2):702-733.
24. Paoli L. Mathematical aspects of vibro-impact problems. In: Leine RI, Acary V, Brüls O, eds. *Advanced Topics in Nonsmooth Dynamics: Transactions of the European Network for Nonsmooth Dynamics*. Springer International Publishing; 2018:135-189.
25. Alessandri A, Coletta P. Design of Luenberger observers for a class of hybrid linear systems. In: Di Benedetto MD, Sangiovanni-Vincentelli A, eds. *Hybrid Systems: Computation and Control*. Springer; 2001:7-18.
26. Zhang J, Zhao X, Zhu F, Karimi HR. Reduced-order observer design for switched descriptor systems with unknown inputs. *IEEE Trans Automat Contr*. 2020;65(1):287-294.
27. Juloski A, Heemels WPMH, Weiland S. Observer design for a class of piecewise linear systems. *Int J Robust Nonlinear Control*. 2007;17(15):1387-1404.
28. van de Wouw N, Pavlov AV. Tracking and synchronisation for a class of PWA systems. *Automatica*. 2008;44(11):2909-2915.
29. Ambrosio L, Fusco N, Pallara D. *Functions of Bounded Variation and Free Discontinuity Problems*. Oxford University Press; 2000.
30. Moreau JJ. Bounded variation in time. In: Moreau JJ, Panagiotopoulos PD, Strang G, eds. *Topics in Nonsmooth Mechanics*. Birkhäuser; 1988:1-74.
31. Glocker C. An introduction to impacts. In: Haslinger J, Stavroulakis GE, eds. *Nonsmooth Mechanics of Solids*. Springer-Verlag; 2006:45-101.
32. Heemels WPMH, Schumacher JM, Weiland S. Linear complementarity systems. *SIAM J Appl Math*. 2000;1997:60.
33. Heemels WPMH, Brogliato B. The complementarity class of hybrid dynamical systems. *Eur J Control*. 2003;9(2-3):322-360.
34. Cottle RW, Pang JS, Stone RE. *The Linear Complementarity Problem*. Classics in Applied Mathematics. Society for Industrial and Applied Mathematics (SIAM); 1992.
35. Murty KG. *Linear Complementarity, Linear and Nonlinear Programming*. Sigma Series in Applied Mathematics. Heldermann Verlag; 1988.
36. Gowda MS, Pang JS. Stability analysis of variational inequalities and nonlinear complementarity problems, via the mixed linear complementarity problem and degree theory. *Math Oper Res*. 1994;19(4):831-879.
37. Heemels WPMH, Camlibel MK, Schumacher JM, Brogliato B. Observer-based control of linear complementarity systems. *Int J Robust Nonlinear Control*. 2011;21(10):1193-1218.
38. Byrnes CI, Lin W. Losslessness, feedback equivalence, and the global stabilization of discrete-time nonlinear systems. *IEEE Trans Automat Contr*. 1994;39(1):83-98.
39. Lozano R, Maschke B, Brogliato B, Egeland O. *Dissipative Systems Analysis and Control: Theory and Applications*. Springer-Verlag; 2000.
40. Nemirovskii A, Gahinet P. The projective method for solving linear matrix inequalities. Proceedings of the 1994 American Control Conference - ACC '94; Vol. 1, 1994:840-844.
41. Khalil HK, Praly L. High-gain observers in nonlinear feedback control. *Int J Robust Nonlinear Control*. 2014;24(6):993-1015.

How to cite this article: Preiswerk PV, Leine RI. State observers for the time discretization of a class of impulsive mechanical systems. *Int J Robust Nonlinear Control*. 2022;1-17. doi: 10.1002/rnc.6168